

Super KEKB/Belle II Project

B. GOLOB(*)

*Faculty of Mathematics and Physics, University of Ljubljana and Jozef Stefan Institute
Ljubljana, Slovenia*

(ricevuto il 14 Settembre 2010; pubblicato online il 12 Gennaio 2011)

Summary. — We present the status of the KEKB accelerator and the Belle detector upgrade, along with several examples of physics measurements to be performed with Belle II at Super KEKB.

PACS 07.05.Fb – Design of experiments.
PACS 14.40.Nd – Bottom mesons.

1. – Introduction

The B factories—the Belle detector taking data at the KEKB collider in KEK [1, 2] and the BaBar detector [3] at the PEP II in SLAC—have in more than a decade of data taking outreached the initial expectations on the physics results. They proved the validity of the Cabibbo-Kobayashi-Maskawa model of the quark mixing and CP violation (CPV). Perhaps even more importantly, they pointed out few hints of discrepancies between the Standard Model (SM) predictions and the results of the measurements. Facing the finalization of the data-taking operations the question thus arises about the future experiments in the field of heavy flavour physics, to experimentally verify the current hints of possible new particles and processes often addressed as the New Physics (NP). Part of the answer are the planned Super B factories in Japan and Italy, that could perform highly sensitive searches for NP, complementary to the long expected ones at the Large Hadron Collider. The so-called precision frontier represented by the two machines requires the achieved luminosities of the B factories to be raised by $\mathcal{O}(10^2)$. In the present paper we summarize the plan and the status of the Belle detector upgrade (Belle II) at the upgraded KEKB (Super KEKB) e^+e^- collider.

In the following section we first briefly discuss the necessary upgrade of the KEKB accelerator. In subsects. 3.1 to 3.3 we summarize the upgrade of the vital parts of the Belle detector—the vertexing, the particle identification system and the electromagnetic

(*) Representing the Belle II Collaboration.

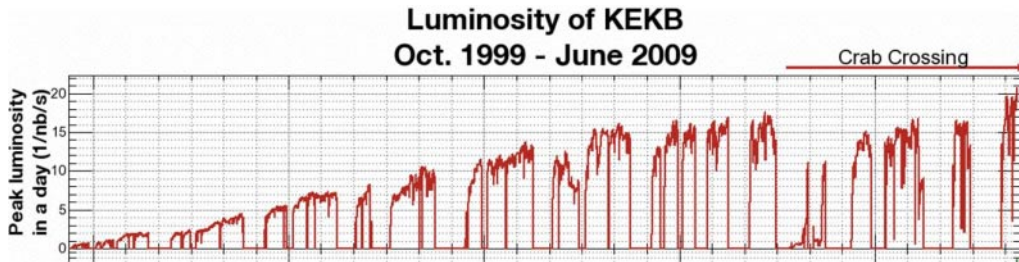


Fig. 1. – Daily peak luminosity of the KEKB collider.

calorimeter, respectively. The upgrade is illustrated with examples of planned measurements that will greatly benefit from the improved collider and detector performance. Finally we draw short conclusions in sect. 4.

2. – From KEKB to Super KEKB

The KEKB accelerator is an asymmetric e^+e^- collider operating at and near the center-of-mass energy of 10.58 GeV, corresponding to the mass of the $\Upsilon(4S)$ resonance. The asymmetry of the beams results in a Lorentz boost factor of $\beta\gamma = 0.425$ which enables the time-dependent measurements in the system of B mesons. The history of the KEKB luminosity is presented in fig. 1. The highest luminosity ever reached in the accelerator ($2.1 \times 10^{34} \text{ cm}^{-2} \text{ s}^{-1}$) is a result of the crab cavities installed in 2007 [4]. The continuous injection scheme and a very stable operation made it possible to collect data corresponding to the integrated luminosity of more than 1 ab^{-1} .

The luminosity of the collider is governed by several factors. The crucial ones for the upgrade of the KEKB are⁽¹⁾ the beam currents (I_{\pm}), the vertical beta function at the interaction point ($\beta_{y\pm}^*$) and the beam-beam parameter $\xi_{y\pm}$. To start from the latter, the beam-beam parameter, $\xi_{y\pm} = \sqrt{\beta_{y\pm}^*/\epsilon_y}$, will remain almost unchanged at Super KEKB, $\xi_{y\pm} \sim 0.1$. The beta function, however, will be extremely reduced: $\beta_{y\pm}^* = 5.9 \text{ mm}/5.9 \text{ mm} \rightarrow 0.27 \text{ mm}/0.41 \text{ mm}$ ⁽²⁾. The emittance will be reduced accordingly to match the current $\xi_{y\pm}$. Both beam currents will be also increased by roughly a factor of two. In terms of the e^+e^- bunches the foreseen upgrade corresponds to the reduction of the current size in direction perpendicular to the beam direction from $\sigma_x \sim 100 \mu\text{m}$, $\sigma_y \sim 2 \mu\text{m}$ to $\sigma_x \sim 10 \mu\text{m}$, $\sigma_y \sim 60 \text{ nm}$. To achieve the desired goal the main tasks during the upgrade will be the installation of longer bending radius in the LER, more arc cells in the HER, re-design of the interaction region with the new final focusing quadrupoles closer to the interaction point, new beam pipe and a new damping ring (see fig. 2). The outstanding problems are a rather small dynamic aperture, larger Touschek background and consequently a shorter lifetime of the beams, directly affecting the luminosity. To cope with these the upgrade includes an increased crossing angle of the two beams (from 22 mrad to 83 mrad) and a slightly smaller asymmetry of the beams (from 3.6 GeV/8 GeV to 4 GeV/7 GeV).

⁽¹⁾ The subscripts \pm denote the high energy electron and the low energy positron beam, HER and LER, respectively.

⁽²⁾ Due to the so-called hourglass effect this requires also a reduction of the $\beta_{x\pm}^*$.

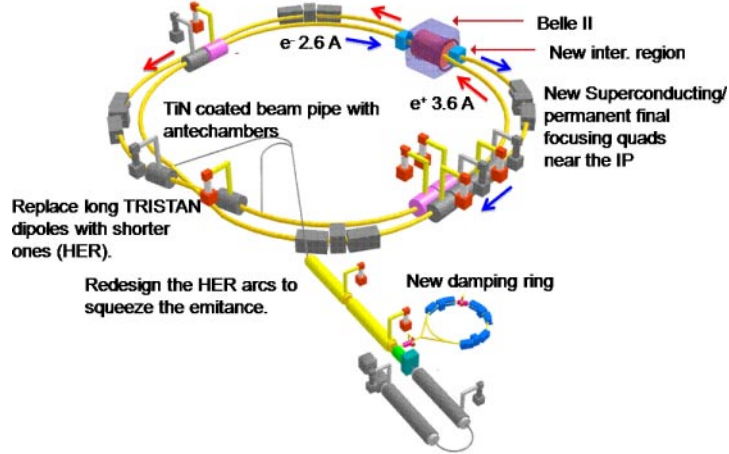


Fig. 2. – The main parts of the KEKB upgrade.

The luminosity of the Super KEKB will reach $\mathcal{L} = 8 \times 10^{34} \text{ cm}^{-2} \text{ s}^{-1}$. Assuming the startup of the machine in 2014, and a rather conservative increase of the starting luminosity to the design value, already in two years of data-taking the available data sample will correspond to 5 ab^{-1} . Integrated luminosity of 50 ab^{-1} is expected in 2020. To illustrate the precision that could be achieved with such a large sample of B meson decays we use the measurement of the lepton forward-backward asymmetry A_{FB} in $B \rightarrow K^* \ell^+ \ell^-$ decays. This observable (or even more so, the zero crossing-point of the $A_{FB}(q^2)$, with $q^2 \equiv m^2(\ell\ell)$) is not very sensitive to the theoretical uncertainties arising from the unknown form factors [5]. In fig. 3 the current Belle measurement [6] is compared to the expected sensitivity at Belle II with $\int \mathcal{L} dt = 5 \text{ ab}^{-1}$. It can be seen that such a measurement will make possible a distinction among various models, for example the SM and the Supergravity models with the reversed sign of the C_7 Wilson coefficient⁽³⁾.

3. – From Belle to Belle II

A rough overview of the Belle detector upgrade is sketched in fig. 4. In the environment of the beams with luminosity of $\mathcal{O}(10^{35}) \text{ cm}^{-2} \text{ s}^{-1}$ the detector will have to cope with an increased background (10–20 times compared to the present), which will be the cause of an increased occupancy and radiation damage. The first level trigger rate is expected to increase from the current 0.5 kHz to around 20 kHz. For several detector components we nevertheless foresee an improved performance and a better overall hermiticity of the detector after the upgrade. The task of vertexing will rely on two layers of DEPFET pixel detectors (PXD) and four layers of double-sided silicon detectors (SSVD). The main tracking device, the Central Drift Chamber (CDC), will have a smaller cell size and an improved read-out system. The particle identification will be performed

⁽³⁾ Note that this specific measurement can also be performed with a high precision at the LHCb. In the following we give examples of measurements that are completely complementary to NP searches at the LHC.

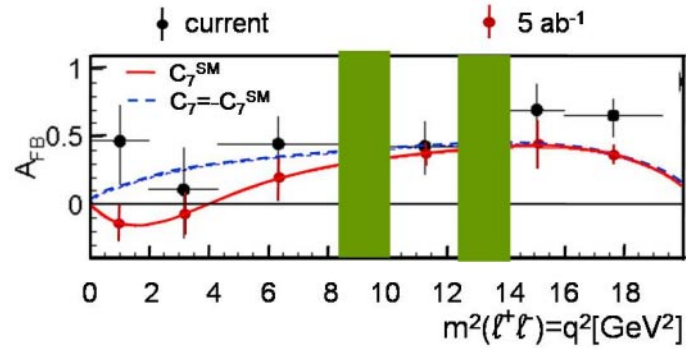


Fig. 3. – The measurement of the lepton forward-backward asymmetry in $B \rightarrow K^* \ell^+ \ell^-$ with 600 fb^{-1} [6] and 5 ab^{-1} data. Shaded regions correspond to the charmonium veto q^2 intervals.

mainly by the Time-of-Propagation counter (TOP) in the barrel and the Rich detector with aerogel radiator (ARICH) in the forward part. For the electromagnetic calorimeter (ECL) the electronics enabling a wave form sampling will be introduced, and some of the current CsI crystals doped with Tl are going to be replaced by the pure CsI. The detector of muons and K_L 's (KLM) will be upgraded with scintillator strips in the endcaps.

3.1. Vertexing. – A schematic view of the future semiconductor detector of Belle II is shown in fig. 5 (left) and is composed of two layers of pixel detectors [7] followed by four layers of double-sided silicon strip detectors. The improvement compared to the current

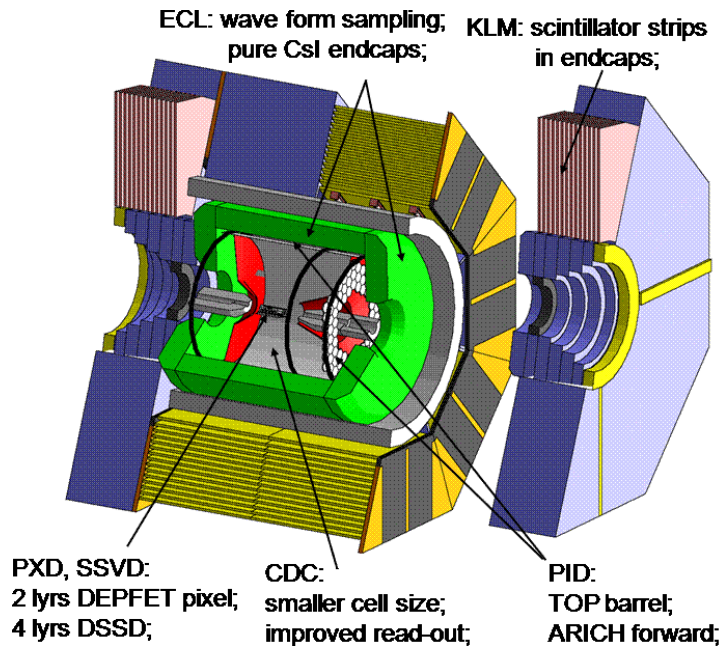


Fig. 4. – The main ingredients of the Belle detector upgrade.

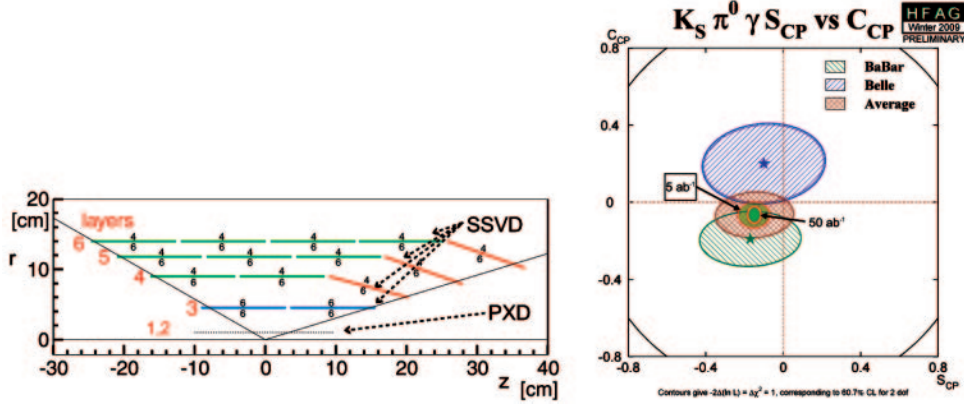


Fig. 5. – Left: A schematic view of the upgraded semiconductor detector. Right: Comparison of the current [10] and expected precision on direct and indirect CPV in $B^0 \rightarrow K_S \pi^0 \gamma$.

detector is twofold: a better spatial resolution of the vertex determination (for around 25% in the case of $B \rightarrow J/\psi K_S$ vertex), and an improved reconstruction efficiency of $K_S \rightarrow \pi^+ \pi^-$ decays with pion signals in the detector, due to the increased radii of the layers. The latter is important for the time-dependent measurements of various decay modes with K_S 's in the final state (increase of around 30%). Since the dependence on the radius of the layers is opposite for the two mentioned improvements a careful optimization of the design was performed.

To illustrate the expected performance, a search for possible right-handed currents in $B^0 \rightarrow K_S \pi^0 \gamma$ is used as a benchmark mode. In these decays only the K_S direction is used together with the interaction point constraint to determine the B meson decay vertex [8]. While the indirect CPV is heavily suppressed in the SM due to the helicity structure of the Hamiltonian, it can be largely increased in some NP models [9]. Figure 5 (right) shows a comparison of the current values of the direct and indirect CPV parameters in this mode [10] with the approximate expected precision including the statistical and systematic uncertainties. While in the Left-Right Symmetric Models S_{CP} can be as high as 0.5, the sensitivity with 50 ab^{-1} of data is smaller than the SM predictions.

3.2. Particle identification. – Particle identification at Belle II will rely on the TOP [11] counter in the barrel part, and ARICH detector in the forward [12]. The TOP detector will consist of a single quartz bar with mirrors on one side and microchannel plate photomultipliers on the other. For high momentum ($3 \text{ GeV}/c$) kaons we expect around 10% better identification efficiency (90–95%) in the barrel at a similar misidentification probability as for the current detector (5% misident. probability).

The particle identification is of course crucial in several measurements, for example the measurements related to the so-called direct CPV puzzle, which arises from the observed difference between the direct CPV asymmetry in $B^0 \rightarrow K^+ \pi^-$ and $B^+ \rightarrow K^+ \pi^0$ decays [13]. While in the explicit calculations of the asymmetries $A_{K\pi}$ several model uncertainties are present, a model-independent sum rule was proposed [14] to test the consistency of the SM. It relates the asymmetries and the branching fractions of several decay modes: $A_{K^+ \pi^-} + A_{K^0 \pi^+} [\mathcal{B}_{K^0 \pi^+} / \mathcal{B}_{K^+ \pi^-}] [\tau_{B^0} / \tau_{B^+}] = A_{K^0 \pi^0} [2\mathcal{B}_{K^0 \pi^0} / \mathcal{B}_{K^+ \pi^-}] + A_{K^+ \pi^0} [2\mathcal{B}_{K^+ \pi^0} / \mathcal{B}_{K^+ \pi^-}] [\tau_{B^0} / \tau_{B^+}]$. Figure 6 (left) shows the

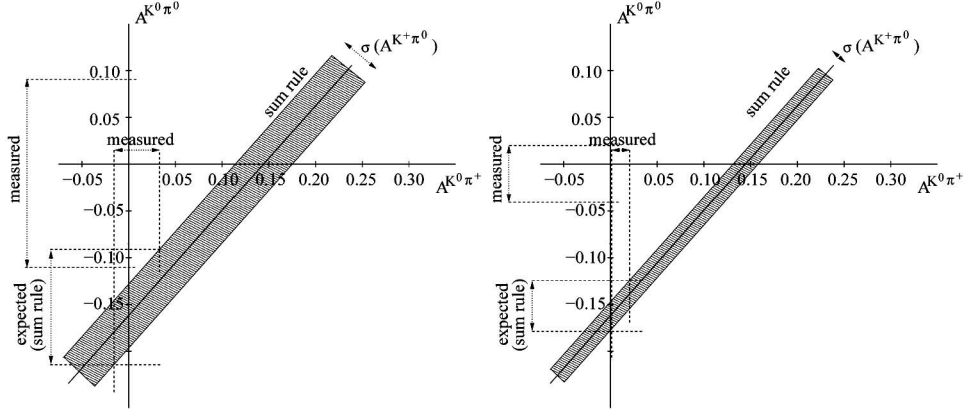


Fig. 6. – Left: direct measurements of $A_{K^0\pi^0}$ and $A_{K^0\pi^+}$ [10] compared to the sum rule [14] prediction. The width of the band is determined by the experimental uncertainties on other quantities entering the sum rule. Right: the same comparison assuming uncertainties expected with 50 ab^{-1} of data.

current status of the measurements using the world average values of the measured observables [10], where $A_{K^0\pi^0}$ is expressed as a function of the $A_{K^0\pi^+}$ using the sum rule. The predictions of the sum rule are in agreement with the direct measurements. With 50 ab^{-1} , and assuming the same central values, a discrepancy between the measurements and the sum rule prediction would be significant (fig. 6 (right)).

3.3. Electromagnetic calorimeter. – In the electromagnetic calorimeter (ECL) upgrade the replacement of the current electronics is foreseen. The new one will enable amplitude-time measurements for the signals in the ECL and will thus help to suppress the background from clusters caused mainly by the off-time beam background (we expect the reduction of this background by a factor of 7). Beside this a partial replacement of the Tl doped CsI crystals with the pure CsI is being under the consideration. Due to the increased rate of backgrounds at Belle II the expected photon detection efficiency of the ECL is around 5–10% lower, while keeping the background at the current level.

The importance of the ECL performance can be best illustrated by the measurement of the $\mathcal{B}(B^+ \rightarrow \tau^+\nu)$ [15]. The method consists of full or partial reconstruction of the tagging B meson, identification of hadrons or charged leptons from the τ decay, and examination of the distribution of the remaining measured energy in the event. For the signal, where the undetected particles are neutrinos, this distribution of energy measured in the ECL peaks at zero. The leptonic B meson decays are interesting since, for example, in the Type II Two Higgs Doublet Models, the SM branching fraction receives a contribution from the charged Higgs boson exchange, expressed as a multiplicative factor: $\mathcal{B}(B^+ \rightarrow \tau^+\nu) = \mathcal{B}^{\text{SM}}[1 - (m_B^2/m_{H^\pm}^2)\tan^2\beta]^2$. With an increased statistical power of the data, and assuming the existing ECL performance, one obtains the five standard deviations discovery region for the charged Higgs boson as shown in fig. 7 [16]. It can be seen that a large area of the $(m_{H^\pm}, \tan\beta)$ -plane (compared to the current exclusion regions) can be covered by this search, especially at larger values of the mass

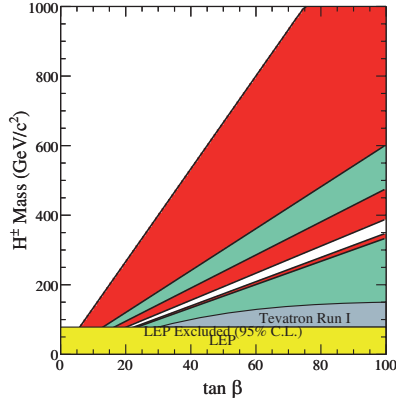


Fig. 7. – (Colour on-line) Five standard deviations discovery region (red, dark shaded) for the charged Higgs boson in the $(m_{H^\pm}, \tan \beta)$ -plane, from the measurement of $\mathcal{B}(B^+ \rightarrow \tau^+ \nu)$ with 50 ab^{-1} [16]. Other shaded regions show the current 95% CL exclusion region.

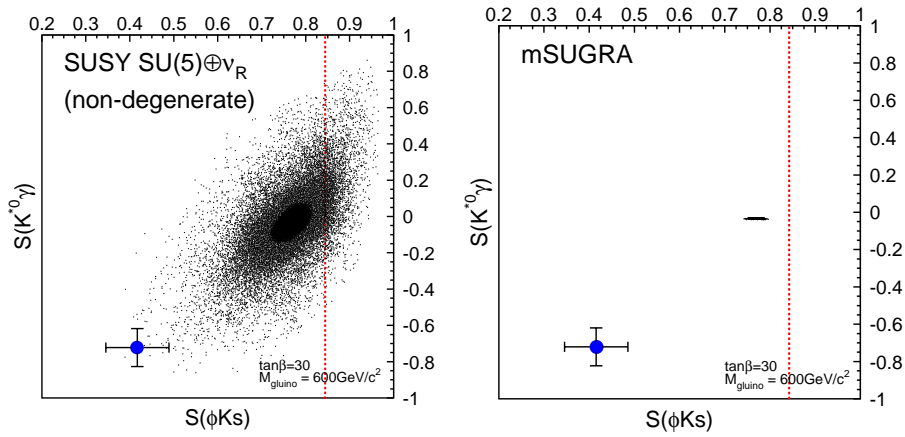


Fig. 8. – Comparison of the correlation between the indirect CPV parameter in $B^0 \rightarrow K^{*0}(\rightarrow K_S \pi^0)\gamma$ and $B^0 \rightarrow \phi K_S$ decays [16] for two models: the minimal supergravity model (mSUGRA) and supersymmetric grand-unification theory with right-handed neutrinos (SUSY $SU(5)$). The points with error bars denote the expected sensitivity at Belle II with 5 ab^{-1} of data.

and $\tan \beta$ ⁽⁴⁾. Such a measurement is to some extent complementary to the measurements of the $b \rightarrow s\gamma$ transition branching fraction which constrain the mass of the charged Higgs boson almost independently of the $\tan \beta$ value.

⁽⁴⁾ In the estimation of the expected sensitivity we also assumed an improvement in the $|V_{ub}|$ and f_B values precision to $\pm 3\%$ each.

4. – Conclusions

In summary, we presented a short overview of the KEKB accelerator and Belle detector upgrade. While technologically most challenging, the preparation of the Super B factory at KEK is well on the way. The key features of the upgrade are illustrated by several measurements that will be possible at Belle II and will represent a highly sensitive search for NP effects, complementary to searches at the LHC. A comprehensive program of physics measurements can be found in [16].

The value of the Super B factory lies not only in a highly sensitive search of NP in individual processes, but to a large extent in the possibility of performing measurements of various observables which through their correlations can help identifying the nature of NP. As an example, fig. 8 [16] shows correlations between the indirect CPV in $B^0 \rightarrow K^{*0}(\rightarrow K_S\pi^0)\gamma$ (see subsect. 3.1) and in the $B^0 \rightarrow \phi K_S$ with the underlying penguin quark process $b \rightarrow s\bar{s}s$ (a naive SM prediction is $S_{\phi K_S} = S_{J/\psi K_S} = \sin 2\phi_1$). In the minimal super gravity model (mSUGRA) and supersymmetric grand-unification theory with right-handed neutrinos (SUSY $SU(5)$) the correlations between the two observables exhibit a different pattern, while the mass spectra of the particles predicted in the two models are similar. If hints of new particles consistent with these predictions arise from the LHC, at Belle II one can distinguish the two models with already $\int \mathcal{L} dt = 5 \text{ ab}^{-1}$ of data.

The preparation of the Belle II detector at Super KEKB is proceeding according to the plan, with the aim of starting the data taking in 2014.

REFERENCES

- [1] ABASHIAN A. *et al.* (BELLE COLLABORATION), *Nucl. Instrum. Methods A*, **479** (2002) 117.
- [2] KUROKAWA S. *et al.*, *Nucl. Instrum. Methods A*, **499** (2003) 1, and other papers in that volume.
- [3] AUBERT B. *et al.* (BABAR COLLABORATION), *Nucl. Instrum. Methods A*, **479** (2002) 1.
- [4] FUNAKOSHI Y., *ICFA Beam Dyn. Newslett.*, **40** (2006) 27.
- [5] See for example BURDMAN G., *Phys. Rev. D*, **52** (1995) 6400; HOVHANNISYAN A., HOU W.-S. and MAHAJAN N., *Phys. Rev. D*, **77** (2008) 014016.
- [6] WEI J.-T. *et al.* (BELLE COLLABORATION), *Phys. Rev. Lett.*, **103** (2009) 171801.
- [7] See for example KEMMER J. and LUTZ G., *Nucl. Instrum. Methods A*, **253** (1987) 356; PERIC I., *Nucl. Instrum. Methods A*, **579** (2007) 685.
- [8] USHIRODA Y. *et al.* (BELLE COLLABORATION), *Phys. Rev. D*, **74** (2006) 111104.
- [9] See for example ATWOOD D. *et al.*, *Phys. Rev. D*, **71** (2005) 076003; GRINSTEIN B. *et al.*, *Phys. Rev. D*, **71** (2005) 011504.
- [10] BARBERIO E. *et al.* (HEAVY FLAVOR AVERAGING GROUP), arXiv:0808.1297, and updates at <http://www.slac.stanford.edu/xorg/hfag/>.
- [11] INAMI K., *Nucl. Instrum. Methods A*, **595** (2008) 96.
- [12] HASHIMOTO S. *et al.*, KEK-REPORT 2004-4.
- [13] LIN S.-W. *et al.* (BELLE COLLABORATION), *Nature*, **452** (2008) 332.
- [14] GRONAU M., *Phys. Lett. B*, **627** (2005) 82; ATWOOD D. and SONI A., *Phys. Rev. D*, **58** (1998) 036005.
- [15] ADACHI I. *et al.* (BELLE COLLABORATION), arXiv:0809.3834.
- [16] AKEROYD A. G. *et al.*, arXiv:1002.5012.